Infantile encephaloneuromyopathy and defective mitochondrial translation due to a homozygous *RMND1* mutation

Beatriz Garcia-Diaz[1], Mario H Barros,[2] Simone Sanna-Cherchi,[3] Valentina Emmanuele,[1] Hasan O Akman,[1] Claudia C Ferreiro-Barros, [4] Rita Horvath,[5] Saba Tadesse,[1] Nader El Gharaby,[6,7] Salvatore DiMauro,[1] Darryl C De Vivo,[1] Aly Shokr,[6] Michio Hirano[1], Catarina M Quinzii[1].

[1]Department of Neurology, Columbia University Medical Center, New York, NY 10032, United States.
[2]Departamento de Microbiologia - ICB-II - Universidade de São Paulo, 05508-900, São Paulo, SP, Brazil
[3]Department of Medicine, Columbia University Medical Center, New York, NY 10032 United States.
[4]Instituto do Cerebro – Hospital Israelita Albert Einstein, 05652-000, São Paulo, SP, Brazil
[5]Mitochondrial Research Group, Institute of Genetic Medicine, Newcastle University, Newcastle upon Tyne, NE1 3BZ, United Kingdom.
[6]Department of Obstetrics and Gynecology, Bugshan General Hospital, PO Box 5860, Jeddah, Saudi Arabia
[7]Current affiliation: Kingston Hospital, Galsworthy Road, London, KT2 7QB, United Kingdom

Address for correspondence and reprints: Dr. Michio Hirano, Columbia University Medical Center, 630 W 168th street, room 423, New York, NY 10032, USA. Telephone: +1-212-305-1048. Fax: +1-212-305-3986. E-mail: mh29@columbia.edu

Words count
Abstract: 207 (max=250)
Main text: 2,036 (references, figures legends and table not included)

Abstract

Defects of mitochondrial protein synthesis are clinically and genetically heterogeneous. We previously described a male infant of consanguineous parents presenting with severe congenital encephalopathy, peripheral neuropathy, myopathy, and lactic acidosis associated with deficiencies of multiple mitochondrial respiratory chain enzymes, and defective mitochondrial translation. In this work, we have characterized four additional affected family members, performed homozygosity mapping, and, in the affected individuals, identified a homozygous splicing mutation in the splice donor site of exon 2 (c.504+1G>A) of required for nuclear meiosis division-1 (*RMND1*). Fibroblasts from affected individuals expressed two aberrant transcripts and had decreased wild-type mRNA and deficiencies of mitochondrial respiratory chain enzymes. The *RMND1* mutation caused haploinsufficiency that was rescued by overexpression of the wild-type transcript in mutant fibroblasts leading to increased levels and activities of mitochondrial respiratory chain proteins. Knockdown of *RMND1* via shRNA recapitulated the biochemical defect of the mutant fibroblasts further supporting a loss-of-function pathomechanism in this disease. RMND1 belongs to the sif2 family, an evolutionary conserved group of proteins sharing the DUF155 domain, with unknown function and never before associated with a human disease. We documented that the protein localizes to mitochondria in mammalian and yeast cells. Further studies are necessary to understand the function of this protein in mitochondrial protein translation.

Main text

Disorders of mitochondrial proteins synthesis, due to mitochondrial or nuclear DNA defects, have been reported in a heterogeneous group of individuals presenting predominantly with prenatal or congenital onset lethal encephalopathies associated with combined deficiencies of respiratory chain and oxidative phosphorylation (OXPHOS) enzymes[1-3]. Mutations in nuclear genes have been described in eight mitochondrial transfer RNA modifying factors[4-13], three mitochondrial ribosomal proteins[14-16], and in three mitochondrial elongation factors[17-22]. Additional mutations have been documented in the gene coding the translational activator of cytochrome *c* oxidase (COX) I (TACO1) (MIM# 612958)[23], and in C12orf65 (MIM#613541), a protein belonging to the family of mitochondrial class I peptide release factors[24].

In 2008, we described an 18 day-old male infant of consanguineous parents from Saudi Arabia with severe neonatal encephaloneuromyopathy and lactic acidosis[1] (individual VI-1 in Figure 1). At birth, the infant was unresponsive, but was successfully resuscitated and intubated. He had little spontaneous limb movements and required mechanical ventilation. Examination revealed prominent tongue fasciculations, bilateral equinus foot deformities, and profound hypotonia of arms and legs. Tendon reflexes were absent. He developed myoclonic jerks and died at age 18 months. A muscle biopsy at age 24 days showed severe COX (complex IV) deficiency. Fibroblasts showed a generalized and severe defect of mitochondrial protein synthesis; reductions of all mitochondrial-translated products; normal mitochondrial transcript levels; reduction in the steady-state levels of complexes I, IV, and V; and normal complex II (encoded

entirely by nuclear genes)[1]. We have now characterized four additional affected family members and we have performed homozygosity mapping in the family (Figure 1). Three affected infants (VI-3, VI-7, and VI-8) had similar presentations with severe neonatal encephaloneuromyopathy evident at birth with lethargy, respiratory failure, profound floppiness, hyporeflexia or areflexia, equinus deformities, lactic acidosis, and death in the first year of life, whereas the fifth affected individual (VI-9) was stillborn without skeletal deformities (Supplemental data Table 1). Deficiencies of multiple mitochondrial respiratory chain enzyme activities were confirmed in individual VI-3 fibroblasts (Table 1).

Informed consent for analyses of biological samples was obtained under a Columbia University Medical Center Institutional Review Board approved protocol. Genomic DNA was purified from blood using standard procedures. To identify areas of shared homozygosity among affected individuals, we performed a high-density genome-wide genotyping of four affected and of eight unaffected relatives using the Illumina 660W-Quad gene chip array, which features over 650,000 markers across the genome (Illumina Inc., San Diego, CA). Clustering, normalization and genotype calls were performed using the dedicated GenomeStudio 2010.3 Genotyping Module (Illumina Inc.). SNP genotypes were analyzed in the PLINK software for standard quality controls[25]. Genome-wide homozygosity mapping, conducted with the Homozygosity Mapper program using default parameters and restricting the analysis to areas of homozygosity shared between all affected individuals, identified a single region of homozygosity shared identical by descent in all the affected (Supplemental data Figure

1A). This region spanned <1Mb between markers rs519861 and rs926777 on chromosome 6q25 and included only seven coding genes (Supplemental data Figure 1B). We sequenced all exons of the seven genes included in the candidate locus by di-deoxy DNA sequencing. All affected individuals were homozygous for a G-to-A transition in the canonical splice donor site of exon 2 (c.504+1G>A) of the long isoform of *RMND1* (NM_017909.2) (Figure 2); parents were carriers; four unaffected siblings were found to be heterozygous, and two homozygous for the wild-type allele. This variant was absent in 210 control allele as well as dbSNP 135 and the "1000 Genomes Project". Primers used to sequence *RMND1* are listed in Supplemental data Table 2.

To evaluate the amount of *RMND1* transcript and protein in individual VI-3 and control fibroblasts, we performed RT-PCR analyses and western blots. RT-PCR analysis of *RMND1* showed 3 splice variants expressed from the mutant allele: 1) the wild-type (31%±1.5), encoding a 449 amino acids protein; 2) a longer transcript (40%± 3.5), with 88 additional nucleotides, leading to the insertion of a premature stop codon at codon 171, 54 amino acids upstream of the start of the only known functional domain of the protein (aa 225-404); and 3) a shorter variant (32%±2.5), in which a cryptic splice site in exon 2 is activated and produces an in-frame deletion of 75 nucleotides (25 amino acids) (Figure 2). In addition, qRT-PCR using a probe that detects all 3 splice variants showed mildly reduced expression of *RMND1* relative to the β-actin (*ACTB)* transcript in individual VI-3 compared with the control (Figure 3A). In accordance with the marked reduction of the wild-type transcript, western blots showed decreased levels of the 52

kDa band corresponding to the expected *RMND1* long isoform and a 28 kDa band in VI-3 fibroblasts compared with controls (Figure 3B-C).

To confirm the pathogenicity of the mutation, we overexpressed *RMND1* in VI-3 and control fibroblasts. Efficiency of overexpression was confirmed by qRT-PCR and western blots (Supplemental data Figure 2). Biochemical activities of mitochondrial respiratory chain enzymes as well as COX and succinate dehydrogenase (SDH) cytochemistry were performed as described[26].

In mutant fibroblasts, *RMND1* cDNA overexpression increased the biochemical activities of mitochondrial enzymes compared to empty vector transfection (Table 1). Specifically, we observed enhanced activities of complexes I+III (55.7%±5.7 after empty vector transfection and 90.7%±5.7 after *RMND1* transfection) and IV (16.3%±4.7 after empty vector transfection and 23.3%±7.1 after *RMND1* transfection) (Figure 4A). Increased COX activity without change in baseline normal SDH activity was confirmed by cytochemistry (Supplemental data Figure 3).

Quantitative evaluation of steady-state level of respiratory chain enzymes subunits by western blot analyses with the Total OXPHOS Complexes Detection Kit cocktail of antibodies (MitoSciences, Eugene, OR, USA) revealed decreased amounts of mitochondrial encoded OXPHOS subunits that increased after transfection with wild-type *RMND1* cDNA. Specifically, after *RMND1* overexpression, there were significant increases in levels of complex I (51.1%±8.0 after empty vector transfection and

71.5%±17 after *RMND1* transfection) and complex IV (47%±8.0 after empty vector transfection and 82%±16 after *RMND1* transfection) in absolute values as well after normalization to SDH as a marker of mitochondrial mass (Figures 4B-C).

To further investigate the function of RMND1, we used shRNA-mediated knockdown of the protein. The clone with the lowest levels of *RMND1* transcript and protein (about 60% of wild-type levels) was chosen to measure respiratory chain and OXPHOS activities, steady-state level and synthesis (Figure 5).

To assess mitochondrial translation, pulse labeling cell cultures from shRNA and control clones was performed as described[1], with slight modifications. Consistent with our observations in mutant fibroblasts, cells with 60% depletion of RMND1 showed decreased activities of complexes I+III (75%) and IV (83%), reduced levels of complexes I (59%) and IV (62%), and diminished mitochondrial proteins synthesis (60%), relative to wild-type cells (Figures 5 A-C).

To assess the potential role of RMND1 in the assembly of ribosomal subunits, we measured 12S and 16S rRNA levels by qRT-PCR. We did not detect any differences in 12S and 16S rRNAs among mutant skin fibroblasts, RMND1-depleted Hela, and corresponding wild-type cells (data not shown).

To confirm the localization of RMND1 in mitochondria of mammalian cells**,** we performed immunohistochemistry and western blots. Fluorescence images, collected

and analyzed by laser scanning confocal microscope showed that the fusion protein co-localizes with mitochondria (Figure 6A). Western blot of isolated cytosolic fraction, endoplasmic reticulum (ER), crude mitochondria, pure mitochondria, and ER-mitochondria from Hela cells showed a 52 kDa band in all fractions, and a 28 kDa band in total cell lysate and in all mitochondrial-containing fractions (Figure 6B). The 28kDa band was absent in both cytosol and ER fraction (Figure 6B). Western blot with anti-YFP antibody (1:1000, 632380, Clontech) of whole 239T cells extracts transfected with a construct encoding YFP-RMND1 fusion protein confirmed the specificity of the two bands, corresponding to the expected long RMND1 isoform (52 kDa) and to the presumably cleaved mitochondrial protein (28 kDa) (Figure 6C).

We generate a disrupted version of *Saccharomyces cerevisiae rmnd1* (*RMND1* homologue) for investigation of mitochondrial function[29]. Mitochondrial fractionation and intra-mitochondrial localization of Ydr282cp with an antibody against the HA epitope were performed as described[30]. Western blot with the anti–HA epitope antibody detected a ~50kDa protein (Supplemental data Figure 4).

In accordance with data on the *ydr282c* mutant strain in the yeast genome collection, yeast containing the *ydr282c* null allele showed a normal phenotype including normal growth in respiration-dependent glycerol medium and mitochondrial protein synthesis (Supplemental data Figure 5).

Mitochondrial proteins synthesis is a complex and still poorly understood process requiring a number of initiation, elongation, and termination factors, all of which are encoded by nuclear genes, together with mtDNA-encoded ribosomal and transfer RNA[31]. Defects in 18 genes directly or indirectly involved in mitochondrial protein synthesis have been described[1,4-25]. In muscle and fibroblasts from an individual with consanguineous parents and a fatal infantile-onset encephalomyopathy with lactic acidosis, we previously demonstrated evidence of a mitochondrial protein synthesis by documenting severe COX deficiency, partially reduced biochemical activities of complexes I and V, normal SDH activity and decreases of all mitochondrial translation products with normal levels of mitochondrial transcripts[1].

Here, we report four additional affected relatives, homozygosity mapping, and identification of a homozygous splice site mutation in the gene encoding the RMND1 protein in all four affected individuals. We have shown that the c.504+1G>A splice donor mutation reduces the wild-type transcript and produces two aberrant transcripts. One alters the reading frame of the protein and produces a prematurely truncated protein with loss of the DUF155 domain. The other is predicted to produce a protein truncated by 25 amino acids. Absence of the truncated protein by western blot with an antibody that recognizes the carboxy-terminus of RMND1 suggests that this aberrant polypeptide is unstable and degraded. These data, together with the results of the RNA interference of the wild-type transcript, showing reduced mitochondrial protein synthesis in partially depleted cells, indicate that the disease is caused by loss, rather than toxic gain, of function. We did not find mutations in *RMND1* in 10 other individuals with

documented defects of mitochondrial protein synthesis[2], suggesting that mutations in *RMND1* may be rare.

RMND1 has at least three isoforms produced by alternative splicing, according with Uniprot: isoform 1, the longest one (449aa), localized to mitochondria[32]; isoform 2 (lacking aa1-211); and isoform 3 (missing aa205-208 DAAN/GTSS and aa209-449). However, in addition to the predicted 52kDa full-length RMND1, western blot revealed a shorter protein (28kDa), which was abundant in purified mitochondrial fractions; therefore, we postulate that the 28kDa RMND1 is the cleaved mitochondrial protein. We sublocalized the yeast homolog, Ydr282c, to the inner mitochondrial membrane with the C-terminus facing the intermembrane space.

RMND1 belongs to the sif2 family, an evolutionary conserved family of proteins with unknown function and sharing the DUF155 domain. The *rmnd1* gene is conserved in species down to yeast. The *S. cerevisiae* orthologue*, YDR282C* has no known functions but has been reported to interact with the functional ortholog of the human Nieman Pick C1 protein, a protein involved in sphingolipid metabolism[33]. Although we showed that the yeast rmnd1 homologue is a mitochondrial protein, yeast null for *rmnd1* are viable in glycerol medium, indicating that respiration in not severely affected. Therefore, either the protein is not involved in yeast mitochondrial protein synthesis or its function overlaps with other proteins in yeast. In fact, divergent functions in yeast and humans have been observed for other mitochondrial proteins, including TACO1, which is required for human COX I mitochondrial translational activation, while the yeast

homolog does not serve this function[23]. Although COX deficiency is prominent in the affected individual's muscle and fibroblasts, the involvement of other respiratory chain/OXPHOS enzymes and the generalized mitochondrial translational defect in mutant fibroblasts and in RMND1 knockdown cells, indicate that RMND1 is not a COX subunit-specific translational activator.

Intriguingly, several RMND*1* homologs seem to be involved in cell division[34], and mitochondrial ribosomal proteins have been shown to be involved in cell cycle regulation[35]. However, against the notion that RMND1 is a structural ribosomal protein are the normal levels of 12S and 16S rRNA in mutant fibroblasts and in RMND1-depleted Hela cells, because mutations in mitochondrial small subunit ribosomal proteins have been shown to decrease 12S rRNA[14,15].

In conclusion, we have identified a novel human mutation affecting a DUF155 protein in a family with a severe autosomal recessive mitochondrial translation defect. Further studies are necessary to understand the function of RMND1 and elucidate its role in mitochondrial protein synthesis.

Supplemental data

Supplemental Data include 2 tables and 5 figures.

Acknowledgments

We are grateful to all of the affected individuals and relatives for their collaboration. The work was partially supported by the Marriott Mitochondrial Disorder Clinical Research Fund (MMDCRF). CMQ is supported by NIH grant K23 HD065871 from the Eunice Kennedy Shriver National Institute Of Child Health & Human Development (NICHD). MH is supported by NIH grants R01 HD057543 and R01 HD056103 from NICHD and the Office of Dietary Supplements (ODS), as well as U54NS078059 from the National Institute of Neurological Disorders and Stroke (NINDS) and NICHD, and a grant from the Muscular Dystrophy Association. MHB and CCFB are supported by Fundacão Amparo a Pesquisa São Paulo (FAPESP). The Authors declare no conflict of interest.

Web resources

URLs for data presented are as follows:

Ensembl Genome browser: www.ensembl.org

Homozygosity Mapper program: http://www.homozygositymapper.org

MitoCarta: http://www.broadinstitute.org/pubs/MitoCarta/human.mitocarta.html

Mitoprot (prediction of mitochondrial targeting sequences):

http://ihg.gsf.de/ihg/mitoprot.html

NCBI dbSNP: www.ncbi.nim.nih.gov/snp

Online Mendelian Inheritance in Man (OMIM): http://www.omim.org/

Universal Protein Resource: www.ebi.ac.uk/uniprot

Yeast Genome database: www.yeastgenome.org

References

1. Ferreiro-Barros, C.C., Tengan, C.H., Barros, M.H., Palenzuela, L., Kanki, C., Quinzii, C., Lou, J., El Gharaby, N., Shokr, A., De Vivo, D.C., et al. (2008). Neonatal mitochondrial encephaloneuromyopathy due to a defect of mitochondrial protein synthesis. J Neurol Sci 275, 128-132.
2. Kemp, J.P., Smith, P.M., Pyle, A., Neeve, V.C., Tuppen, H.A., Schara, U., Talim, B., Topaloglu, H., Holinski-Feder, E., Abicht, A., et al. (2011). Nuclear factors involved in mitochondrial translation cause a subgroup of combined respiratory chain deficiency. Brain 134, 183-195.
3. Rotig, A. (2011). Human diseases with impaired mitochondrial protein synthesis. Biochim Biophys Acta 1807, 1198-1205.
4. Bykhovskaya, Y., Casas, K., Mengesha, E., Inbal, A., and Fischel-Ghodsian, N. (2004). Missense mutation in pseudouridine synthase 1 (PUS1) causes mitochondrial myopathy and sideroblastic anemia (MLASA). Am J Hum Genet 74, 1303-1308.
5. Fernandez-Vizarra, E., Berardinelli, A., Valente, L., Tiranti, V., and Zeviani, M. (2007). Nonsense mutation in pseudouridylate synthase 1 (PUS1) in two brothers affected by myopathy, lactic acidosis and sideroblastic anaemia (MLASA). J Med Genet 44, 173-180.
6. Riley, L.G., Cooper, S., Hickey, P., Rudinger-Thirion, J., McKenzie, M., Compton, A., Lim, S.C., Thorburn, D., Ryan, M.T., Giege, R., et al. (2010). Mutation of the

mitochondrial tyrosyl-tRNA synthetase gene, YARS2, causes myopathy, lactic acidosis, and sideroblastic anemia--MLASA syndrome. Am J Hum Genet 87, 52-59.

7. Scheper, G.C., van der Klok, T., van Andel, R.J., van Berkel, C.G., Sissler, M., Smet, J., Muravina, T.I., Serkov, S.V., Uziel, G., Bugiani, M., et al. (2007). Mitochondrial aspartyl-tRNA synthetase deficiency causes leukoencephalopathy with brain stem and spinal cord involvement and lactate elevation. Nat Genet 39, 534-539.

8. Isohanni, P., Linnankivi, T., Buzkova, J., Lonnqvist, T., Pihko, H., Valanne, L., Tienari, P.J., Elovaara, I., Pirttila, T., Reunanen, M., et al. (2010). DARS2 mutations in mitochondrial leucoencephalopathy and multiple sclerosis. J Med Genet 47, 66-70.

9. Edvardson, S., Shaag, A., Kolesnikova, O., Gomori, J.M., Tarassov, I., Einbinder, T., Saada, A., and Elpeleg, O. (2007). Deleterious mutation in the mitochondrial arginyl-transfer RNA synthetase gene is associated with pontocerebellar hypoplasia. Am J Hum Genet 81, 857-862.

10. Zeharia, A., Shaag, A., Pappo, O., Mager-Heckel, A.M., Saada, A., Beinat, M., Karicheva, O., Mandel, H., Ofek, N., Segel, R., et al. (2009). Acute infantile liver failure due to mutations in the TRMU gene. Am J Hum Genet 85, 401-407.

11. Steenweg, M.E., Ghezzi, D., Haack, T., Abbink, T.E., Martinelli, D., van Berkel, C.G., Bley, A., Diogo, L., Grillo, E., Te Water Naudé, J., et al. (2012). Leukoencephalopathy with thalamus and brainstem involvement and high lactate 'LTBL' caused by EARS2 mutations. . Brain 135, 1387-1394.

12. Bayat, V., Thiffault, I., Jaiswal, M., Tétreault, M., Donti, T., Sasarman, F., Bernard, G., Demers-Lamarche, J., Dicaire, M.J., Mathieu, J., et al. (2012). Mutations in the mitochondrial methionyl-tRNA synthetase cause a neurodegenerative phenotype in flies and a recessive ataxia (ARSAL) in humans. . PLoS Biol 10.

13. Pierce, S.B., Chisholm, K.M., Lynch, E.D., Lee, M.K., Walsh, T., Opitz, J.M., Li, W., Klevit, R.E., and King, M.C. (2011). Mutations in mitochondrial histidyl tRNA synthetase HARS2 cause ovarian dysgenesis and sensorineural hearing loss of Perrault syndrome. Proc Natl Acad Sci U S A 108, 6543-6548.

14. Miller, C., Saada, A., Shaul, N., Shabtai, N., Ben-Shalom, E., Shaag, A., Hershkovitz, E., and Elpeleg, O. (2004). Defective mitochondrial translation caused by a ribosomal protein (MRPS16) mutation. Ann Neurol 56, 734-738.

15. Saada, A., Shaag, A., Arnon, S., Dolfin, T., Miller, C., Fuchs-Telem, D., Lombes, A., and Elpeleg, O. (2007). Antenatal mitochondrial disease caused by mitochondrial ribosomal protein (MRPS22) mutation. J Med Genet 44, 784-786.

16. Galmiche, L., Serre, V., Beinat, M., Assouline, Z., Lebre, A.S., Chretien, D., Nietschke, P., Benes, V., Boddaert, N., Sidi, D., et al. (2011). Exome sequencing identifies MRPL3 mutation in mitochondrial cardiomyopathy. Hum Mutat 32, 1225-1231.

17. Coenen, M.J., Antonicka, H., Ugalde, C., Sasarman, F., Rossi, R., Heister, J.G., Newbold, R.F., Trijbels, F.J., van den Heuvel, L.P., Shoubridge, E.A., et al. (2004). Mutant mitochondrial elongation factor G1 and combined oxidative phosphorylation deficiency. N Engl J Med 351, 2080-2086.

18. Antonicka, H., Sasarman, F., Kennaway, N.G., and Shoubridge, E.A. (2006). The molecular basis for tissue specificity of the oxidative phosphorylation deficiencies in patients with mutations in the mitochondrial translation factor EFG1. Hum Mol Genet 15, 1835-1846.

19. Smeitink, J.A., Elpeleg, O., Antonicka, H., Diepstra, H., Saada, A., Smits, P., Sasarman, F., Vriend, G., Jacob-Hirsch, J., Shaag, A., et al. (2006). Distinct clinical phenotypes associated with a mutation in the mitochondrial translation elongation factor EFTs. Am J Hum Genet 79, 869-877.

20. Smits, P., Antonicka, H., van Hasselt, P.M., Weraarpachai, W., Haller, W., Schreurs, M., Venselaar, H., Rodenburg, R.J., Smeitink, J.A.v., and an den Heuvel, L.P. (2011). Mutation in subdomain G' of mitochondrial elongation factor G1 is associated with combined OXPHOS deficiency in fibroblasts but not in muscle. European journal of human genetics : EJHG 19, 275-279.

21. Vedrenne, V., Galmiche, L., Chretien, D., de Lonlay, P., Munnich, A., and Rotig, A. (2011). Mutation in the mitochondrial translation elongation factor EFTs results in severe infantile liver failure. . Journal of hepatology 56, 294-297.

22. Valente L, Tiranti V, Marsano RM, Malfatti E, Fernandez-Vizarra E, Donnini C, Mereghetti P, De Gioia L, Burlina A, Castellan C, et al. (2007). Infantile encephalopathy and defective mitochondrial DNA translation in patients with mutations of mitochondrial elongation factors EFG1 and EFTu. American journal of human genetics 80, 44-58.

23. Weraarpachai, W., Antonicka, H., Sasarman, F., Seeger, J., Schrank, B., Kolesar, J.E., Lochmuller, H., Chevrette, M., Kaufman, B.A., Horvath, R., et al.

(2009). Mutation in TACO1, encoding a translational activator of COX I, results in cytochrome c oxidase deficiency and late-onset Leigh syndrome. Nat Genet 41, 833-837.

24. Antonicka, H., Ostergaard, E., Sasarman, F., Weraarpachai, W., Wibrand, F., Pedersen, A.M., Rodenburg, R.J., van der Knaap, M.S., Smeitink, J.A., Chrzanowska-Lightowlers, Z.M., et al. (2010). Mutations in C12orf65 in patients with encephalomyopathy and a mitochondrial translation defect. Am J Hum Genet 87, 115-122.

25. Purcell, S., Neale, B., Todd-Brown, K., Thomas, L., Ferreira, M.A., Bender, D., Maller, J., Sklar, P., de Bakker, P.I., Daly, M.J., et al. (2007). PLINK: a tool set for whole-genome association and population-based linkage analyses. Am J Hum Genet 81, 559-575.

26. DiMauro, S., Servidei, S., Zeviani, M., DiRocco, M., DeVivo, D.C., DiDonato, S., Uziel, G., Berry, K., Hoganson, G., Johnsen, S.D., et al. (1987). Cytochrome c oxidase deficiency in Leigh syndrome. Ann Neurol 22, 498-506.

27. Stone, S.J., and Vance, J.E. (2000). Phosphatidylserine synthase-1 and -2 are localized to mitochondria-associated membranes. J Biol Chem 275, 34534-34540.

28. Hill, J.E., Myers, A.M., Koerner, T.J., and Tzagoloff, A. (1986). Yeast/E. coli shuttle vectors with multiple unique restriction sites. Yeast 2, 163-167.

29. Rothstein, R.J. (1983). One-step gene disruption in yeast. . Methods Enzymol 101, 202-211.

30. Barros, M.H., Johnson, A., Gin, P., Marbois, B.N., Clarke, C.F., and Tzagoloff, A. (2005). The Saccharomyces cerevisiae COQ10 gene encodes a START domain protein required for function of coenzyme Q in respiration. J Biol Chem 280, 42627-42635.

31. Smits, P., Smeitink, J., and van den Heuvel, L. (2010). Mitochondrial translation and beyond: processes implicated in combined oxidative phosphorylation deficiencies. J Biomed Biotechnol 2010, 737385.

32. Pagliarini, D.J., Calvo, S.E., Chang, B., Sheth, S.A., Vafai, S.B., Ong, S.E., Walford, G.A., Sugiana, C., Boneh, A., Chen, W.K., et al. (2008). A mitochondrial protein compendium elucidates complex I disease biology. Cell 134, 112-123.

33. Costanzo, M., Baryshnikova, A., Bellay, J., Kim, Y., Spear, E.D., Sevier, C.S., Ding, H., Koh, J.L., Toufighi, K., Mostafavi, S., et al. (2010). The genetic landscape of a cell. Science 327, 425-431.

34. Zhou, X., Li, Q., Chen, X., Liu, J., Zhang, Q., Liu, Y., Liu, K., and Xu, J. (2011). The Arabidopsis RETARDED ROOT GROWTH gene encodes a mitochondria-localized protein that is required for cell division in the root meristem. Plant Physiol 157, 1793-1804.

35. Yoo, Y.A., Kim, M.J., Park, J.K., Chung, Y.M., Lee, J.H., Chi, S.G., Kim, J.S., and Yoo, Y.D. (2005). Mitochondrial ribosomal protein L41 suppresses cell growth in association with p53 and p27Kip1. Mol Cell Biol 25, 6603-6616.

Figures Titles and Legends

Figure 1. Pedigree of the family. Black symbols represent affected individuals; open symbols, unaffected relatives; small black symbols, stillborns; diagonal lines, deceased persons; and asterisk, DNA available.

Figure 2. *RMND1* has 4 splicing variants of which only 3 encode proteins: ENST00000367303 (12 exons, isoform 1 [I1]), ENST00000367303 (11 exons, I2), and ENST00000444024 (9 exons, I3). All 3 coding variants contain DUF155 domain indicated by purple boxes. Coding regions are represented by blue boxes and non-coding regions by white boxes. The longest transcript has a predicted N-terminal 33 amino acid mitochondrial targeting sequence (MTS). Agarose gel showing PCR product of *RMND1* cDNA from control (C) and VI-3 fibroblasts (VI-3).
L indicates the 100 base-pair DNA ladder. The splice site mutation c.504+1G>A (arrow) produces 2 aberrant transcripts (AT1 and AT2) and reduces amount of wild-type transcript (middle band). The longer transcript, AT1, includes insertion of 88 nucleotides after exon 2 and generates a premature stop at codon 171. In the shorter variant, AT2, a cryptic splice-site in exon 2 is activated, resulting in an in-frame deletion of 75 nucleotides and a protein 25 amino acids shorter than the wild-type.

RNA was extracted using PureLink RNA Mini Kit (Ambion®, Austin, TX), reverse transcribed into cDNA with the VILO RT-PCR kit (Invitrogen, Grand Island, NY), and reverse transcriptase-PCR (RT-PCR) of exons 2-7 was performed. The RT-PCR products were electrophoresed in 2% agarose gels.

Figure 3. RMND1 is partially reduced in VI-3 fibroblasts. A) Reverse transcriptase quantitative PCR to characterize the expression level of *RMND1* mRNA in VI-3 fibroblasts. Real-time quantitative RT-PCR (qRT-PCR) was performed using TaqMan® Assays for *RMND1* and *ACTB* (β-actin) transcripts (Applied Biosystems). B-C) Western blot to measure the level of RMND1 in VI-3 fibroblasts. Proteins were extracted and concentrations were measured with the BCA Protein Assay Kit (Pierce). Five µg of protein were electrophoresed in a SDS-12%-PAGE gel, transferred to Immun-Blot® PVDF membranes (Biorad, Hercules, CA, USA) and probed with rabbit polyclonal anti-RMND1 antibody (product # HPA031399, Sigma-Aldrich, St Louis, MO) at 1:1,000 dilution. Mouse monoclonal anti-actin antibody (Sigma-Aldrich) was used at 1:10,000 dilution. Protein–antibody interaction was detected with peroxidase-conjugated goat anti-mouse IgG antibody (1:5000) (Sigma-Aldrich), using SuperSignal® chemi-luminiscence detection kit (Thermo Fisher Scientific, Waltham, MA). Quantitation of the bands was performed by densitometric analysis using the NIH ImageJ software package (version 1.45). Values are expressed as percentages of controls and are the results of at least 3 different experiments. C1-4, controls; actin, β-actin. The asterisk (*) indicates Student's t test $P<0.05$.

Figure 4. Complementation analysis in VI-3 and control fibroblasts. After transient transfection with a construct encoding wild-type RMND1, mutant cells showed increased biochemical activities of mitochondrial respiratory chain enzymes normalized to citrate synthase (CS) (A), and increase in mitochondrial OXPHOS subunits steady state level (B-C). Values reflect the results of at least 3 different transfection

experiments and are expressed as percentage of not transfected control. The asterisk (*) indicates Student's t test $P<0.05$.

Figure 5. Effects of *RMND1* knockdown in Hela cells. Hela cells were cultured in DMEM with 10% FBS until 70–80% confluent. Transfection with scramble shRNA-pLKO plasmid (negative control) and *RMND1*-specific TRC shRNA-pLKO plasmid construct (TRCN0000135730, Sigma Aldrich) was mediated by Lipofectamine 2000 (Invitrogen). Five hours after transfection, cells were selected with Puromycin in DMEM 2% FBS and transfected clones were individually expanded in DMEM 10% FBS. *RMND1* knock-down was assessed in 30 clones by qRT-PCR and western blot.

A) Mitochondrial respiratory chain enzymes activities; B) Western blot analysis of mitochondrial respiratory enzymes steady-state levels, and C) pulse labeling with [^{35}S] methionine of mitochondrial proteins. Five x10^5 cells cultured in 10 cm culture plates were washed in methionine-free DMEM and subsequently incubated in the same medium supplemented with 15% dialyzed FBS, 1.2mM sodium pyruvate, and glucose for 30 minutes. Cytosolic protein synthesis was inhibited by addition of emetine (0.1µg/µl) for 7 minutes at 37 °C. Mitochondrial proteins were labeled with 50µCi [^{35}S]-methionine Redivue (Amersham Biosciences, Piscataway, NJ) in methionine-free medium, and incubated for 1 hour at 37 °C. After treatment, cells were incubated for 10 min in DMEM supplemented with 10% FBS, and collected by scraping. Protein aliquots (15 µg per sample) were electrophoresed in a 4-12% Bis-Tris polyacrylamide gradient gel for 4 hours at 85V. The gel was dried for 60 minutes at 80 °C and analyzed with a phosphorimager.

The seven subunits of complex I (ND), three subunits of complex IV (COX), and two subunits of complex V (ATP) are indicated at the left. Values are expressed as percentages of control. An asterisk (*) indicates Student's t test $P<0.05$; (**) indicates Student's test t $P<0.01$.

Figure 6. RMND1 localization in mammalian cells by immunohistochemistry (A) and quantitation by Western blot (B). *RMND1* cDNA was amplified from a commercial vector containing the human full-length cDNA using *Bam*HI restriction enzyme recognition site integrated forward 5'-AGG ATC CGC CAT GCC AGC CAC ACT CCT CAG AGC CG and *Age*I restriction enzyme recognition site integrated reverse 5'-CGA CCG GTG ATT TCA TGG TTG GAA GGT GTG primers. PCR product was digested with *Bam*HI and *Age*I and cloned into pEYFP expression vector, in-frame and upstream of YFP coding sequence. Fidelity of the fusion RMND1-YFP construct in the expression vector was verified by sequencing and 2.5 μg were used to transiently transfect HEK293T cells as described above. Culture media were supplemented with 0.1 μM MitoTracker Red (Invitrogen) for 30 minutes before fixing the cells with 4% formalin-PBS to detect mitochondria. Purification of mitochondria and cellular fractions was performed as previously described[27] and western blot was performed using the following antibodies: anti-RMND1 (1:1000, Sigma), anti-Complex II (1:5000, MitoScience, Abcam, Cambridge, MA), anti-APH1a (1:1000, Abcam), and anti-Vinculin (1:5000, Sigma-Aldrich, St. Louis, MO); peroxidase-conjugated anti-rabbit (1:2000) or anti-mouse IgG (1:5000) secondary antibodies (Sigma-Aldrich). Cellular fractions were isolated from Hela cells: 25 μg of protein from the total lysate (L), and equal amounts (6 μg) from

each fraction: cytoplasmic fraction (CF), endoplasmatic reticulum (ER), crude mitochondria (CMt), pure mitochondria (PMt) and ER/mitochondria (ERMt) were loaded onto the gel. The known molecular masses (in kilodaltons [kDa]) of proteins used to confirm cell fraction enrichment are indicated in the left margin of the gel. C) Western blot of total HEK293T cells extracts transfected with YFP-RMND1 fusion protein with anti-GFP-antibody confirmed the specificity of the 2 bands detected by the anti-RMND1 antibody.

Table 1. Mitochondrial respiratory chain enzyme activities in VI-3 and control (C) fibroblasts after transient transfection with empty vector (e.v.) and after transient transfection with a construct encoding RMND1 isoform 1.

Complex	VI-3	C	VI-3 e.v.	C e.v.	VI-3 *RMND1*	C *RMND1*
IV/CS	0.06±0.002	0.69±0.02	0.11±0.07	0.59±0.44	0.14±0.08	0.5±0.41
II+III/CS	0.05±0.001	0.11±0.03	0.02±0.01	0.05±0.02	0.03±0.02	0.04±0.02
I+III/CS	1.1±0.88	2.59±0.07	0.98±0.79	1.75±0.77	1.46±0.59	1.80±1.29

Activity expressed in µmol/min/mg proteins and normalized to citrate synthase. Values represent the mean ± SD of at least three different experiments, and three different transfections.

Complex IV, cytochrome *c* oxidase (COX); complexes II+III, succinate cytochrome *c* reductase; complexes I+III, nicotinamide dehydrogenase (NADH) cytochrome *c* reductase; and citrate synthase (CS).

Figure 1

Click here to download high resolution image

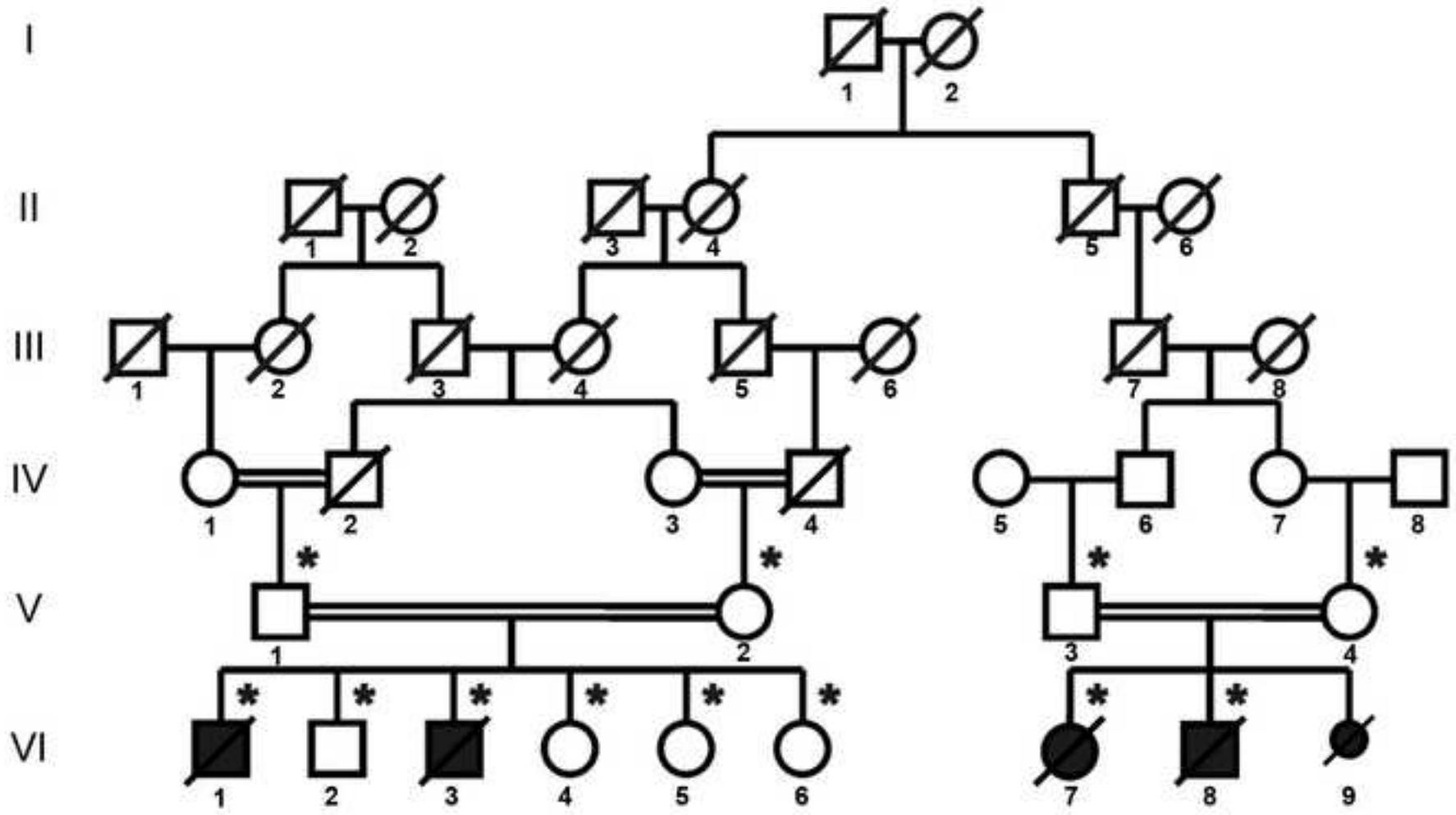

Figure 2

Click here to download high resolution image

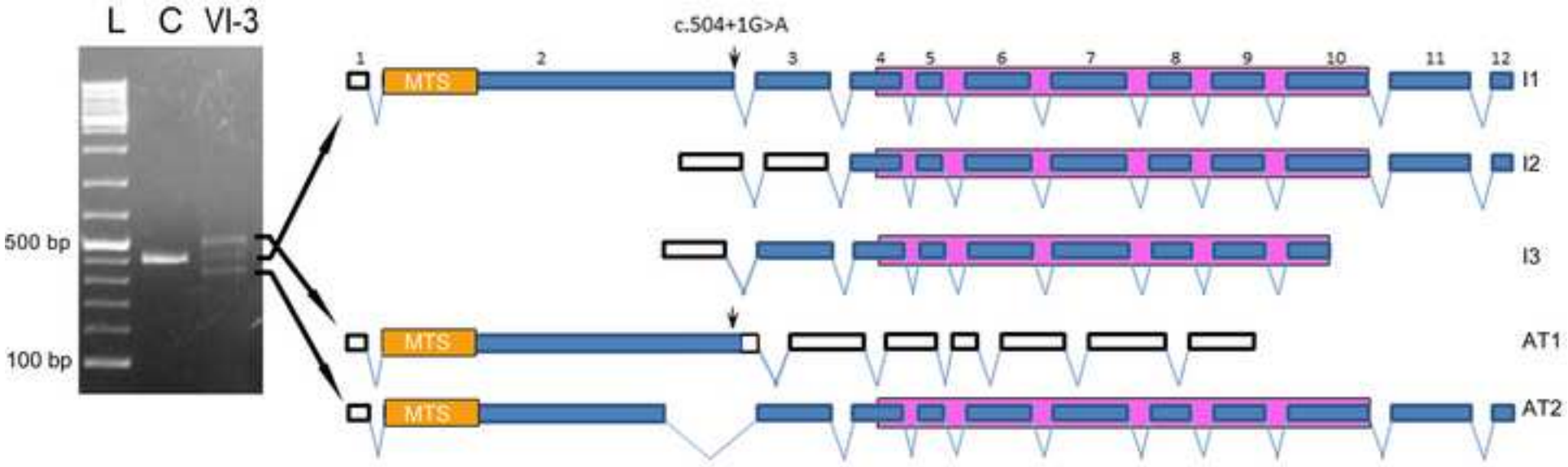

Figure 3

Click here to download high resolution image

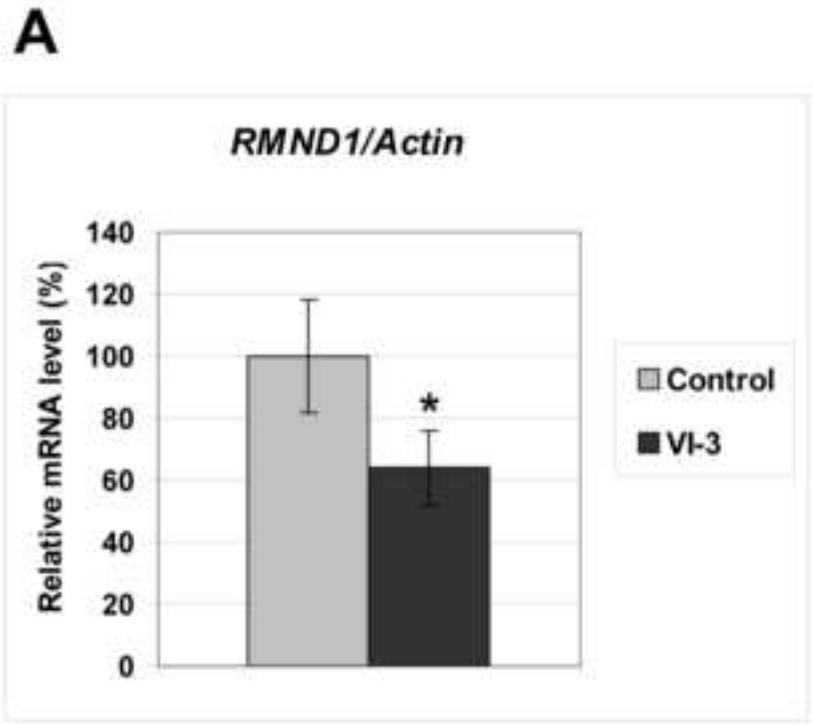

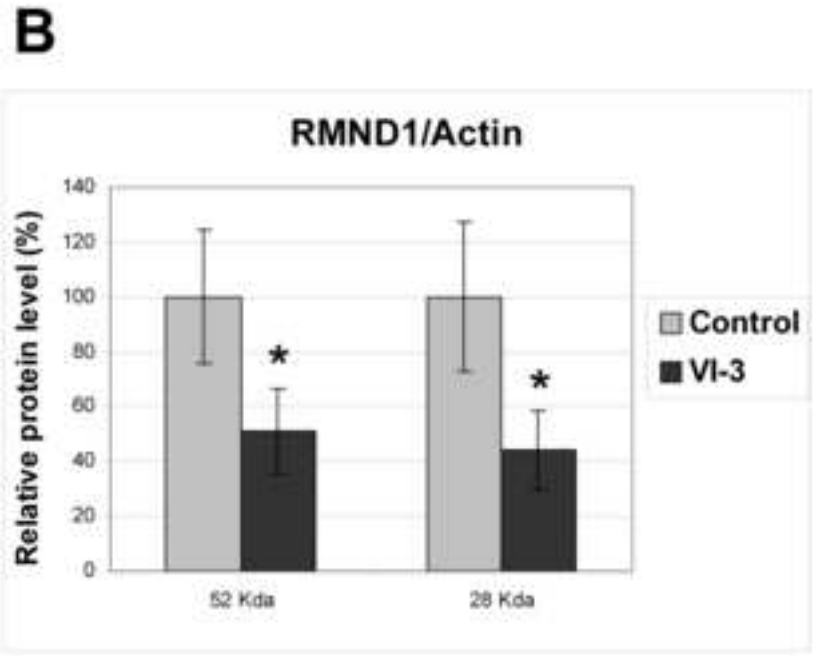

Figure 4

Click here to download high resolution image

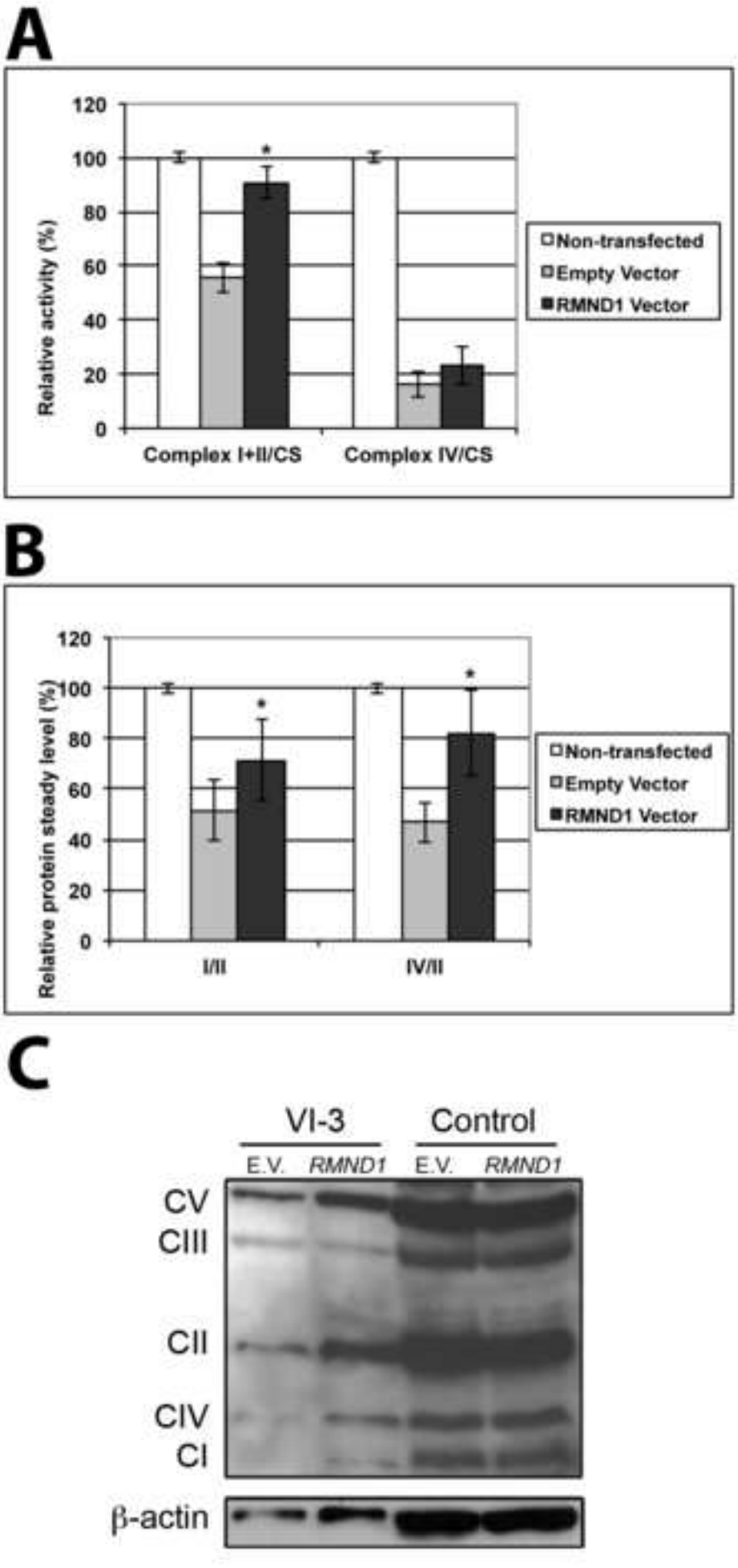

Figure 5

Click here to download high resolution image

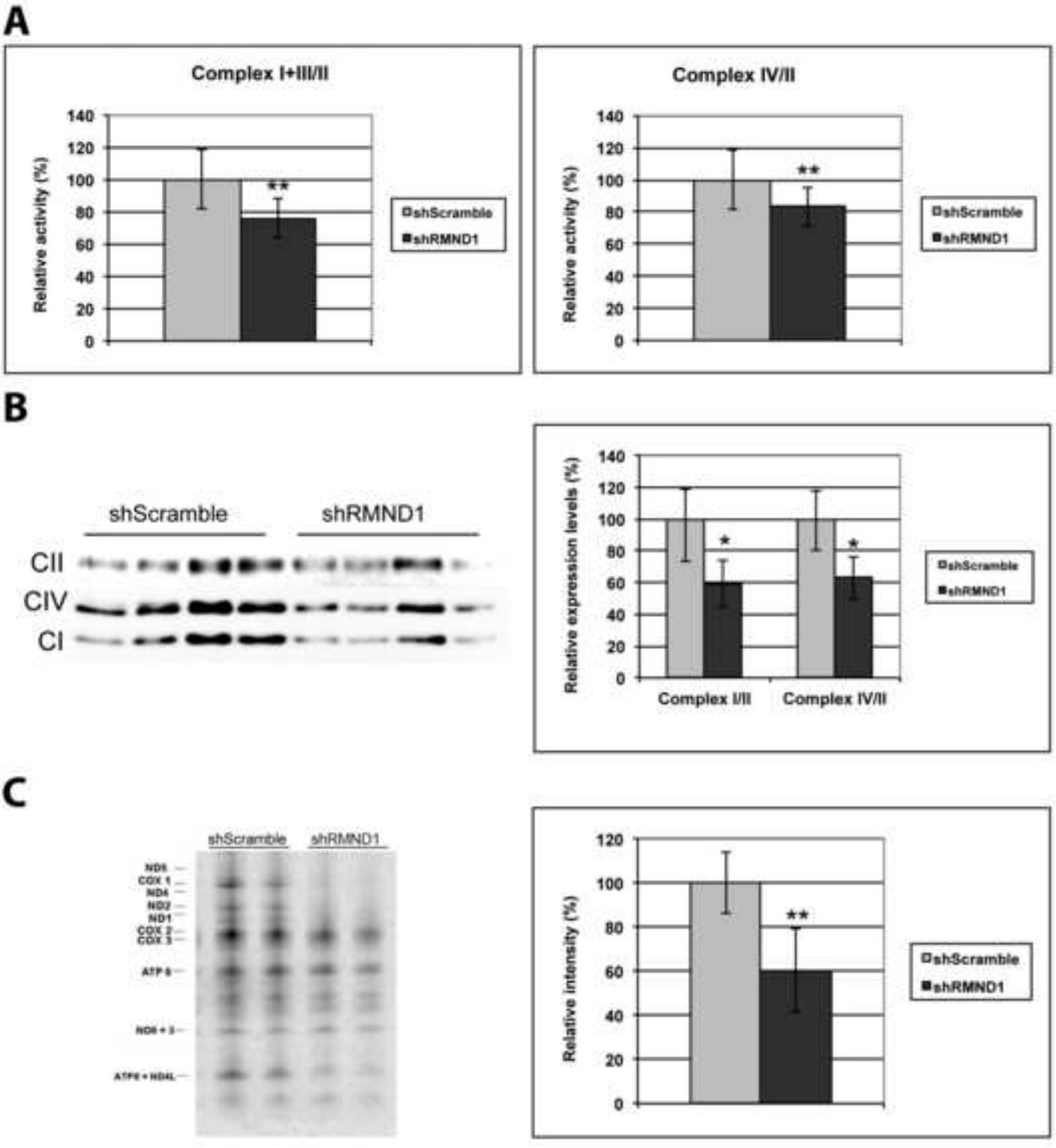

Figure 6

Click here to download high resolution image

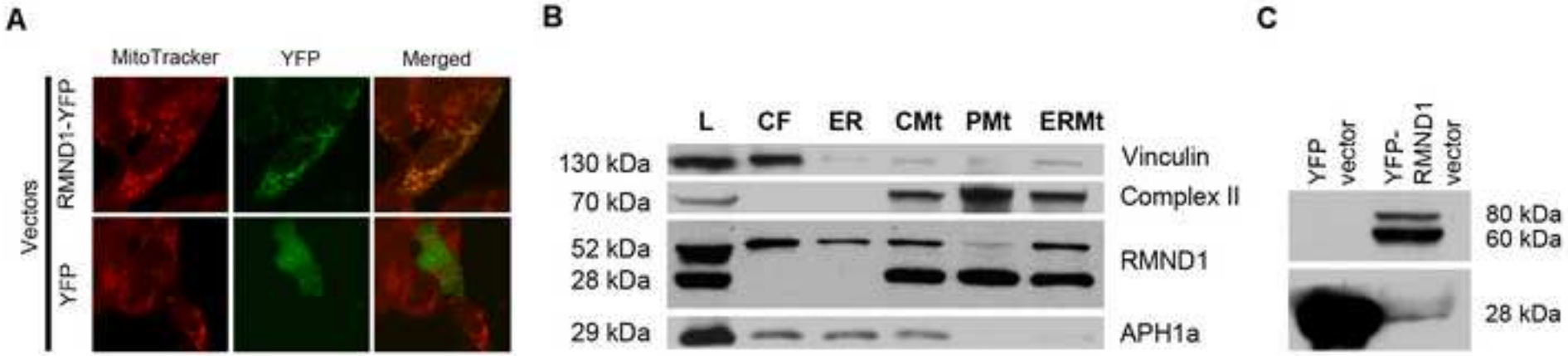

Supplement:

Supplemental Figure 1:

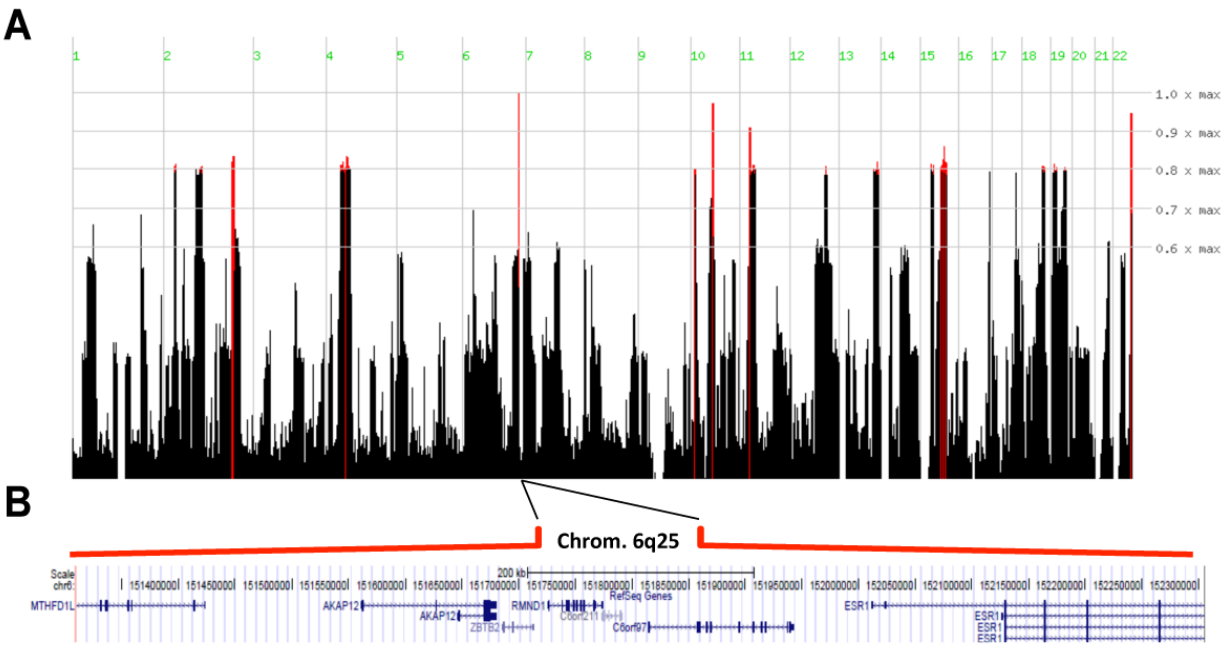

Supplemental Figure 2:

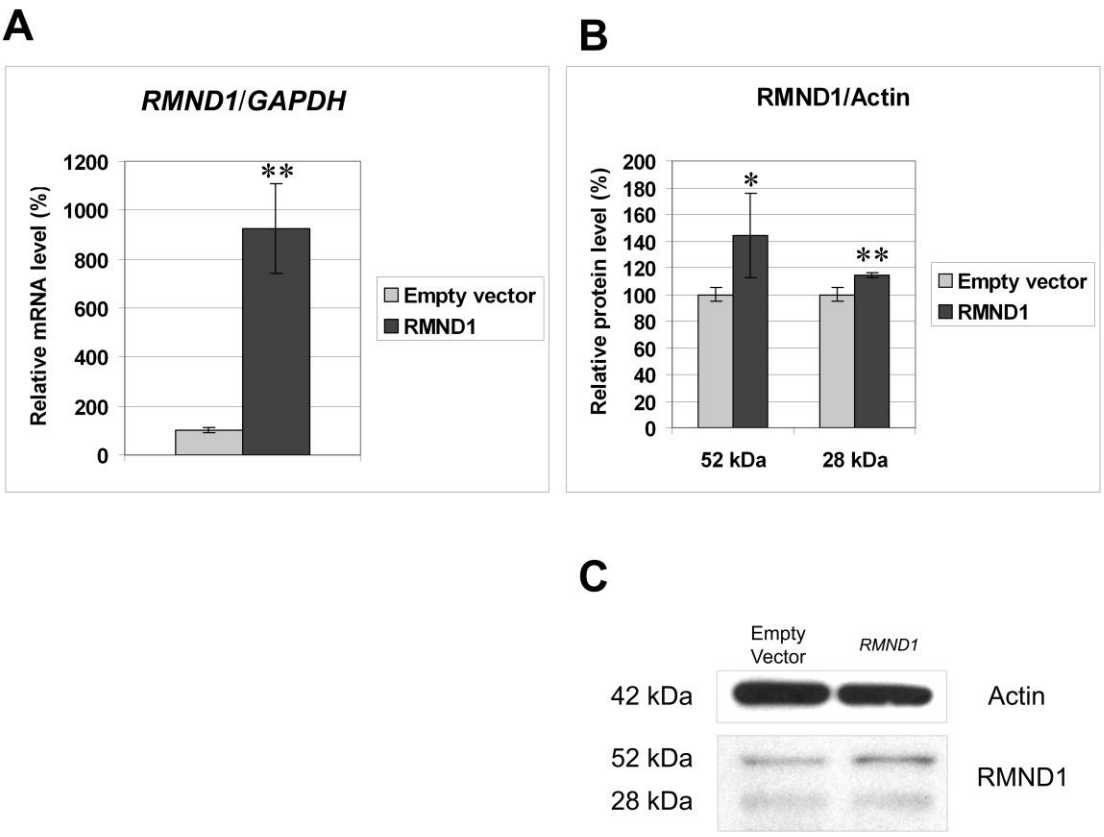

Supplemental Figure 3:

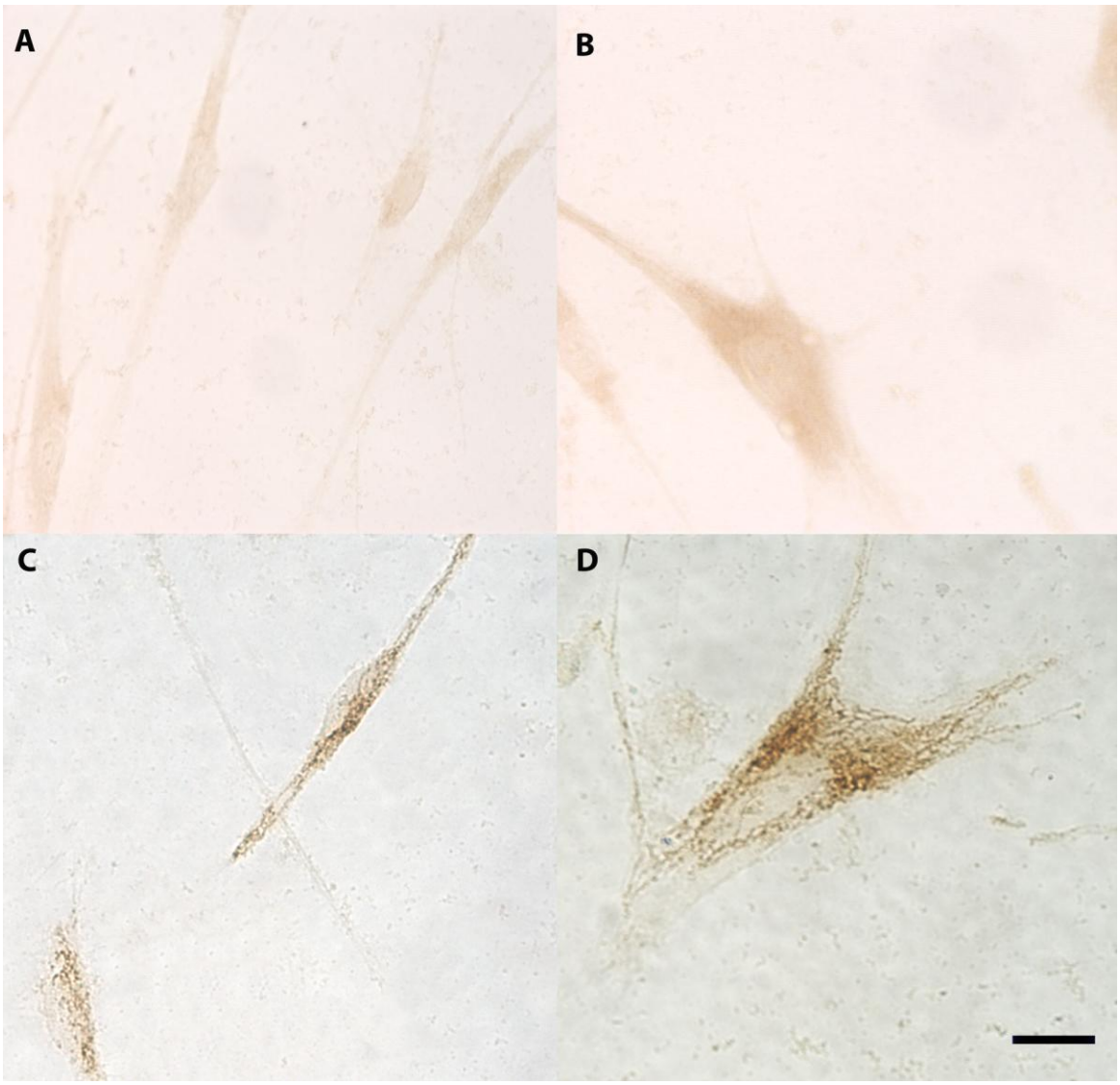

Supplemental Figure 4:

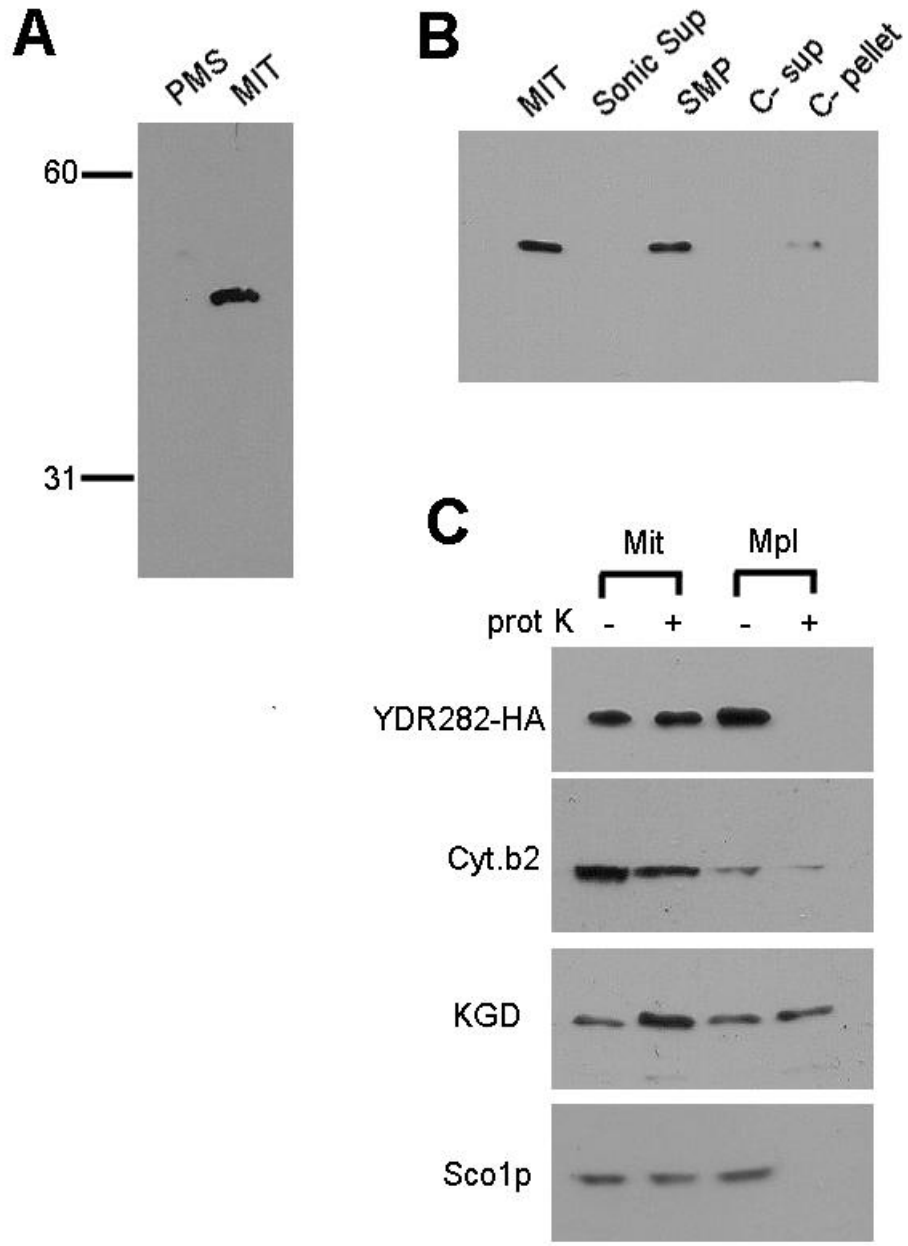

Supplemental Figure 5:

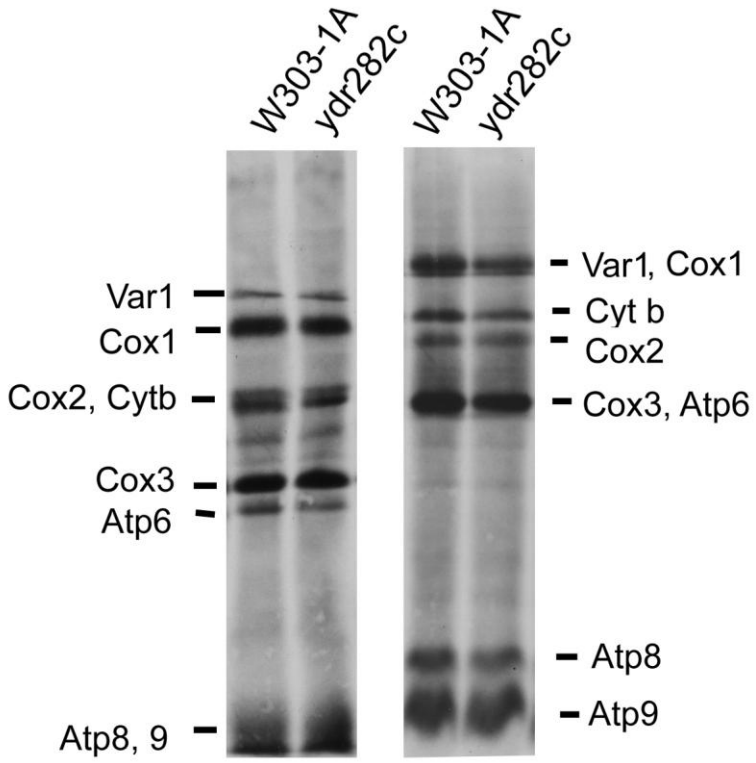

Supplemental Tables

Supplemental Table 1. Clinical presentation of the 5 affected subjects studied.

GA, gestational age; C-section, cesarean section; CPD, Cephalopelvic Disproportion; NA, not available; CPR, cardiopulmonary resuscitation.

#	Sex	GA (weeks) / birth weight	Pregnancy / Delivery	Assisted ventilation at birth	Clinical data	Blood lactate (normal 0.5-2.2mM)	Age at death
VI-1	Male	40 / 3.20 Kg	C-section	Yes (mechanic ventilation)	Little spontaneous limb movement, prominent tongue fasciculations, bilateral equinus deformities of the feet, profound hypotonia of arms and legs, absent tendon reflexes myoclonic jerks at day 3.	3.2 mM	18 months
VI-3	Male	34 / 1.99 Kg	Antepartum hemorrhage due to placenta previa / C-section	Yes (mechanic ventilation)	Lethargic, floppy, hyporeflexic, generalized hypotonia, bilateral equines feet deformity.	3.5 mM	12 days
VI-7	Female	38 / 2.86 Kg	Mild polyhydramnios / C-section due to CPD	Yes (mechanical ventilation)	Floppy, absent Moro reflex, normal pupillary light reflex, hypotonia (proximal>distal) tongue fasciculations, muscular skeletal deformities (bilateral hyperextended knees, bilateral talipes equinovarus)	2.5-8.4 mM	8 months
VI-8	Male	38 / 2.88 Kg	Uneventful / Vaginal delivery	Yes (mechanic ventilation)	Lethargic, floppy, hyporeflexic, generalized hypotonia, bilateral equines feet deformity.	5.7mM	4 months
VI-9	Female	34 / 2.01 Kg	Polyhydramnios / NA	CPR attempted	No skeletal deformities	NA	Stillborn

Supplemental Table 2. PCR primers used to amplify human *RMND1* (annealing temperature: 59 °C)

Exon	Forward (5' → 3')	Reverse (5' → 3')
2	GGCAAAGTGGCAGAAACACT	CTCTTACGTTGGCGGTAAGG
3	GAATGGAGTCCAGTAGGGTG	CCACCTCAAGTAATAATGATCC
4	AGATGGTGATTGTGTTACAGAG	CACAATTACTTGACCCAAACC
5	ACCCTAAAGAATGTATTCCATC	AATTTCCCTTCTAATGTTTCAG
6	CCTTTTCCTTAAAAACATGCAA	TGCACACCTGTACTCCCACT
7	GTCAAAATGACCTCCAGAAAG	TCCCTCAGTGAAATGACAAC
8	GCGATTCAGTTTCCTCTATCC	AGATTCTGGTATCCAGTGGG
9	GCCCTGTTGACCTAATGC	ACTATGGGAATGTTTTCTTGAG
10	GGGTAACATAGCAAGACCCTC	GTACAGAGGACAAGAAGGGG
11	CTTTGGGGAGAGGACTGAG	GCCCCTGTATTTGTGAAAAG
12	CAATTCATAGGTTGCCACG	TCCTGATCTCATCTCAAGCC
cDNA	GCCGAAGAATCGGTCATCTA	AGTGATGCTTCCCAAATTGC

Supplemental Figure Legends

Supplemental Figure 1. Genome-wide homozygosity mapping identified a single region of homozygosity due to shared identity by descent in all affected patients (A). The region on chromosome 6q25 spanned <1Mb between the markers rs519861 and rs926777 and included only 7 coding genes (B).

Supplemental Figure 2. Quantitative PCR to assess transcripts levels (A) and western blot to determine protein levels as determined by ratios of RMND1/β-actin bands (B) and western blots showing 52 and 28 kDa bands detected by anti-RMND1 antibody (C) to assess transfection efficiency of a construct encoding RMND1 in VI-3 fibroblasts. The full-length human *RMND1* cDNA cloned in the pCMV-SPORT6 vector was generated with the Open Bio system (Thermo Fisher Scientific), and fidelity of the final product was confirmed by sequencing. Cells were cultured in high glucose DMEM medium supplemented with 10% FBS (Invitrogen). When 70% confluent, cells were transiently transfected with 5 µg of wild-type *RMND1* or empty CMV-SPORT6 vector plus Lipofectamine 2000 (Invitrogen) in FBS-free medium. After 5 hours, cells were cultured in high-glucose medium supplemented with 2% FBS for 24 hours. The asterisk (*) indicates Student's t test $P<0.05$; (**) indicates Student's t test $P<0.01$.

Supplemental Figure 3**.** Transient expression of *RMND1* cDNA increases cytochrome *c* oxidase (COX) activity. Cytochemical assessment of COX activity in VI-3 fibroblasts before (A and B), and after transient transfection with a *RMND1* expression vector (C and D). Three COX-positive cells are evident in the field. Scale bar represents 20 µm.

Supplemental Figure 4. Subcellular localization of the yeast homolog (Ydr282p) of human *RMND1* in the mitochondrial inner membrane. After PCR amplification of the *Ydr282c* ORF with the oligonucleotides 5'-ggcctgcagtcaagcgtagtctgggacgtcgtatgggtactttgtagcatctagatc and 5'-

cctttaaagatctgtgcggcg, the PCR product was digested with *Bgl*II and *Pst*I and ligated into YEp351 previously digested with the same enzymes. The recombinant plasmid was used to transform *W303ΔYDR282c* and generated YDR282p with a C-terminal HA tag. Western blot with the anti–hemaglutinin (HA) antibody detected a ~50kDa protein (A). HA-tagged Ydr282p is present in the mitochondrial (MIT), but not post-mitochondrial supernatant (PMS) (A). Post-sonic disruption of mitochondria, the protein was recovered predominantly in the membrane fraction (sub-mitochondrial particles [SMP]) and was not extracted with carbonate (C-sup) with a partial recovery in post-carbonate pellet (C-pellet) indicating strong association of Ydr282p with membranes (B). The HA-tagged protein was susceptible to proteinase K in mitoplasts (Mpl) but not in mitochondria (Mit) indicating that the C-terminus protrudes into the intermembrane space (C). Cyt b_2 is a mitochondrial intermembrane space protein; α-ketoglutarate dehydrogenase (KGD) is a matrix protein; and Sco1p is an inner membrane protein.

Supplemental Figure 5. Mitochondrial protein synthesis in wild-type (W303-1A) and *rmnd1*-null (Δydr282c) *S. cerevisiae* strain. To generate a disrupted version of *Saccharomyces cerevisiae rmnd1* (*RMND1* homologue), ORF YDR282c was PCR-amplified from total yeast nuclear DNA with primers 5'-cctttaaagatctgtgcggcg and 5'- cccctgcagtttagatccgagattcc. The 1756 bp fragment containing the gene flanked by 305 nucleotides of 5'-untranslated and 224 nucleotides of 3'-untranslated sequences was digested with *Bgl*II and *Pst*I, and then transferred to *YEp352* and *YIp352*[28]. The recombinant plasmid (pDR282/ST1) was digested with *Bcl*I, then the 725bp *Bcl*I internal fragment was replaced by a 1.1 kb fragment containing the yeast *HIS3* gene. The *YDR282:HIS3* allele was isolated from this plasmid (pDR282/ST8) as a linear 2.1 kb *Sac*I-*Pst*I fragment, which was used to replace the wild-type gene in the respiratory competent haploid strain W303-1A by homologous recombination. Histidine-independent transformants were

shown to have the null allele by PCR and restriction analysis, confirming the successful construction of W303ΔYDR282.

To assess mitochondrial protein synthesis, the parental *Saccharomyces cerevisiae* strain W303-1A and the *rmnd1*-null mutant (Δydr282c) were grown at 28 °C and incorporation of ^{35}S-methionine into the mitochondrial translation products was assayed *in vivo* after inactivation of cytosolic translation with cycloheximide. The cells were labeled at room temperature for 10 min. Total cellular proteins were separated by SDS-PAGE on a 17% polyacrylamide gel with a 30:0.8 ratio of acylamide to bis-acrylamide, and on a 12% acylamide gel with 6M urea to separate Cox3p and Atp6p. Proteins were transferred to nitrocellulose and exposed to X-ray film. The respective positions of the yeast mitochondrial translational products: Var1, Cox1, Cyt b, Cox2, Cox3, Atp6, Atp8, and Atp9 are indicated.